XVI International Conference on Durability of Building Materials and Components
DBMC 2023, China
K.F. Li and D.P. Fang (Eds)

Recycling of Silty Waste Soil by CO_2 Treatment for Construction Block Manufacture

Yao Du[1,2] **and Qiang Zeng**[1]

[1] College of Civil Engineering and Architecture, Zhejiang University, 310058 Hangzhou, PR China, 22212051@zju.edu.cn (Yao Du), cengq14@zju.edu.cn (Qiang Zeng)

[2] Shenergy Environmental Technology Co., Ltd, 311121, PR China

Abstract. *The poor engineering performance of silty waste soil (SWS) seriously restricts its utilization in new constructions that, in turn, need a large amount of building materials. Meanwhile, traditional sintering technology of clay brick production is prohibited due to its high CO_2 emissions. In the present work, a rapid CO_2 mineralization method is proposed to treat SWS with active lime after the pressing forming process of building block manufacturing. The optimum mix proportion and pressing forming parameters of SWS blocks are presented. Microstructure of selected SWS block samples is characterized by mercury intrusion porosimetry (MIP) and X-ray computed tomography (XCT), and mineral changes are analyzed by X-rays diffraction (XRD). CO_2 emissions from the SWS block production are evaluated considering the entire manufacturing process. Overall, the present study provides a proof-of-concept path that enables recycling of SWS for construction block production with low CO_2 emissions.*

Keywords: *CO_2 curing; Non-sintering technology; Compressive strength; CO_2 emissions*

1 Introduction

The continuous urbanization in coastal areas of China has produced massive SWS that occupies land resources and pollutes the environment (Zhang et al. 2023). To tackle this issue, various methods have been proposed to recycle SWS for sintering bricks and ceramsite, and subgrade materials, and landscaping (Song et al. 2021). While the sintering techniques can greatly mitigate the shortages of SWS with fine particle size and high organic content, the consequent high energy consumption and carbon emissions (Chen et al. 2013) cannot meet the urgent needs of China's urban green and sustainable development policy (Huang et al.2022).

Carbon mineralization (CM) technique could be used to improve the engineering performance of SWS, promoting its utilization. In fact, the practice of using alkaline substances to react with CO_2 to generate carbonate minerals to bind particles has a history of thousands of years (Yang et al. 1985). When adding appropriate amount of alkaline substances to soil, it can react with CO_2 in the air, which acts as a binder to improve the soil structure (Wang et al. 2021, Gajurel et al. 2021, Puppala et al. 2016). Furthermore, the studies have found that using CM technology to produce different carbonate minerals in soil can caused an increase in unconfined compressive strength, improving the stability of soil surface (Sun et al. 2022, Keykha et al. 2021, Wang et al. 2019). Additionally, Inasaka et al. (2021) used CM tests to reveal the CO_2 capture amount in alkaline sludge, and found that when the addition of quicklime was 3%, the CO_2 capture rate reached 90.0%.

The above researches enlighten that it is prospective to develop the environment-friendly SWS-based composite with superior mechanics regulation by CM with simple pressing molding. This study aims at (1) understanding the CM mechanisms in tightly compacted solids,

(2) optimizing the mix ratios and producing process.

2 Materials and methods

2.1 Raw materials

SWS was obtained from Oufei reclamation area in Wenzhou, China. The chemical composition of SWS is shown in table 1, which was analyzed by X-ray fluorescence (XRF, Bruker S8 TIGER of Bruker Co., Ltd, Germany). Calcium hydroxide ($Ca(OH)_2$, AR) was purchased from Titan Corporation Ltd (Shanghai, China). The chemical composition of fine aggregate (FA, medium sand) used in this study was mainly silica, with a fineness modulus of 2.66.

Table 1. Chemical composition of SWS.

Compositon	SiO_2	CaO	Al_2O_3	Fe_2O_3	K_2O	MgO	Na_2O
Content of SM (wt %)	53.4	4.14	17.6	5.61	3.17	2.26	0.796

2.2 Sample preparation

The SWS block studied in this paper needed to be formed by pressing and CM treatment. To optimize ratios and parameters of the producing process, three types of pressures (1, 5, and 10 MPa) and three kinds of FA/SSC ratios (0, 1, and 2) were designed. The mass ratio of $Ca(OH)_2$ to dry SWS was controlled to a constant value (1:4). The amount of water added was 25mass% of dry SWS and 5mass% of dry FA to obtain a state suitable for compression molding. The detailed mix proportions of this study are shown in Table 2.

Table 2. Mix proportions of the SWS blocks.

Sample name	FA/SSC	Forming pressure /(MPa)	calcium hydroxide /(kg/t)	SWS /(kg/t)	FA / (kg/t)
S0-1	0:1	1	200.00	600.00	0.00
S0-5	0:1	5	200.00	600.00	0.00
S0-10	0:1	10	200.00	600.00	0.00
S1-1	1:1	1	108.70	326.08	434.78
S1-5	1:1	5	108.70	326.08	434.78
S1-10	1:1	10	108.70	326.08	434.78
S2-1	2:1	1	74.63	223.89	597.05
S2-5	2:1	5	74.63	223.89	597.05
S2-10	2:1	10	74.63	223.89	597.05

The producing process is as follows. Dry SWS was first blended with $Ca(OH)_2$ and then the mixture of SWS and $Ca(OH)_2$ (SSC) was mixed with different ratios (0-200 mass%) of FA. The dry powder materials were stirred with tap water in a mortar mixer, and then compacted under different pressures (1, 5 and 10 MPa) with a rectangular-shaped mold (40 mm × 40 mm × 100 mm). The specimens were treated in a carbonization reactor under a CO_2 pressure of 0.5 MPa for 12 hours, and finally dried in air at 353.15 K for 24 h before testing. The above

experimental process is shown in Fig. 2.

Fig. 1. Production flow chart for SWS blocks.

2.3 Characterization

After CM treatment, the compressive strength was determined at a loading rate of 1.0kN/s with a universal testing machine (NYL-600 of Wu Xi Jian Yi Instrument&Machinery Co., Ltd., Wu Xi, China). In the compressive strength test, three parallel specimens were measured each time for the same material.

The following analyses were conducted under the crushed specimens. Mineral composition was analyzed by X-ray diffraction (XRD, Bruker D8 Advance of Bruker Co., Ltd, Germany) with a stepped scan covering angles of 5°–90° (2θ) at a scanning speed of 6°/min respectively; microstructure was investigated by X-ray computed tomography (XCT, XTH 225/320 LC of Nikon Co., Ltd., Japan) with the accelerating voltage of 120 kV and the beam current of 80 μA, and mercury intrusion porosimetry (MIP, IV 9510 of Micromeritics Co., Ltd., Georgia, USA) with the maximum applied pressure of 60000 psi and equilibrium time of 10 s.

3 Results and discussion

3.1 Engineering properties of SWS block

Fig. 3 shows the strength values of SWS blocks before and after CM treatment under different FA/SSC ratios and forming pressures. The following features can be observed:

(1) The compressive strength of SWS blocks without CM treatment increased significantly with the increase of forming pressure. When the forming pressure was increased to 5 MPa, the strength of S0-5-R block rapidly increased to 4.06 MPa, by 136% (Fig. 2a). However, the impact of forming pressure on the strength of SWS blocks decreased after CM treatment.

(2) The compressive strength first increased and then decreased with increase of the FA/SSC ratios and the highest strength was obtained when the FA/SSC ratio was 1 in all forming pressures.

(3) CM can significantly improve the strength of SWS blocks, especially for the samples with low forming pressure. The strength of S0-1-C block was 5.43 MPa, 3.71 MPa higher than

that of S0-1-R one, with an increase of 2.16 times.

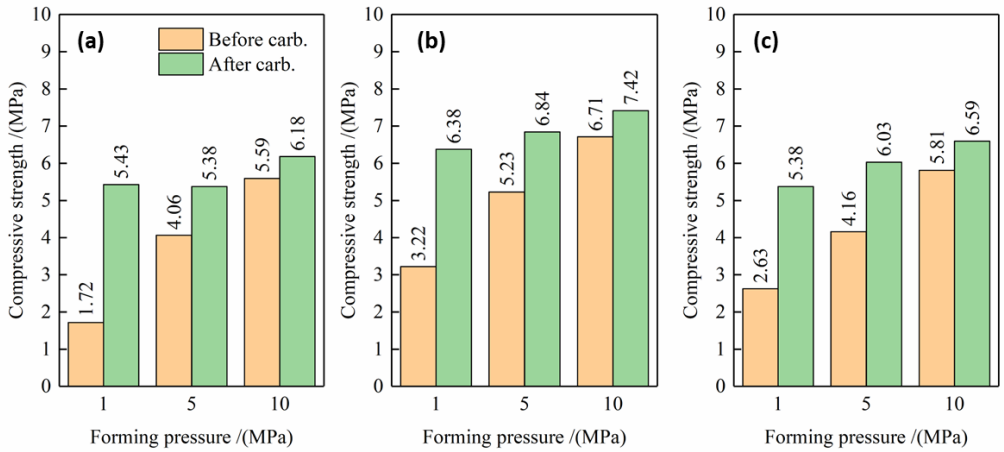

Fig. 2. Strength of the blocks with different forming pressures and FA/SSC ratios before and after carbonization: (a) FA/SSC = 0, (b)FA/SSC = 1, (c) FA/SSC = 2.

3.2 Chemical outcomes

Fig. 3 shows the XRD patterns of internal and external areas of S1-1, S1-5 and S1-10 samples. The most obvious characteristic spectrum in the results (Fig. 3a) is quartz crystal (Quartz), but the intensity of spectra of $Ca(OH)_2$ crystal (Portlandite) and $CaCO_3$ crystal (Calcite) is relatively weak.

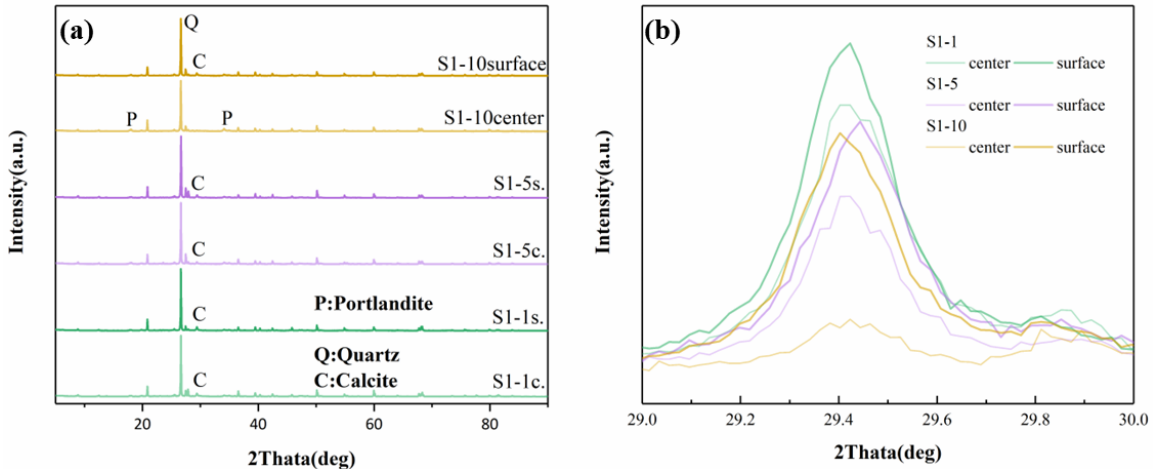

Fig. 3. XRD patterns of internal and external areas of the SWS blocks with different molding pressures under the FA/SSC ratio of 1: (a) a range 2θ of 5-90° ; (b) a range 2θ of 29-30°.

Focusing on the range of 29-30° (Fig. 3b), it can be observed that under different molding pressures, the characteristic peaks of $CaCO_3$ were more obvious on the outer layer of samples, indicating that the outer layer is carbonized with higher degree. In the internal areas of SWS blocks, the characteristic peaks decreased with the increase of molding pressure, and S1-10 sample basically had no $CaCO_3$ characteristic peaks, manifesting that substantial carbonization

has not occurred in the center of samples. This result is consistent with the basic process of carbonization reaction, which usually starts from the surface of samples. As CO_2 gradually diffuses into the sample, the degree of carbonization reaction increases gradually. The denser the sample, the slower the CO_2 transport process, and the lower the corresponding degree of carbonization reaction (Abanades et al. 2017). Thus, it is difficult for CO_2 to diffuse into the inside of S1-10 sample with narrow pores, resulting in insufficient carbonization reaction.

3.3 Microstructure

Fig. 4 shows the XCT images of S1-5 and S1-10 samples before and after CM treatment. When the molding pressure increased to 10 MPa, the pore density in blocks decreased, and the XCT total porosity was 0.37%. This is because the gaps between particles are gradually squeezed under high pressure, leading to gradual compression of the pores (Wu et al. 2021). As a result, these compressed pores may not be detected by XCT. After CM treatment, XCT analysis showed a decrease in 3D pore density. The total porosity of S1-5 sample decreased from 1.01% to 0.73%, by 28%. Similarly, the porosity of S1-10 sample decreased from 0.37% to 0.25%, by 33%. This indicates that CM treatment can significantly reduce the porosity and improve the compactness of blocks.

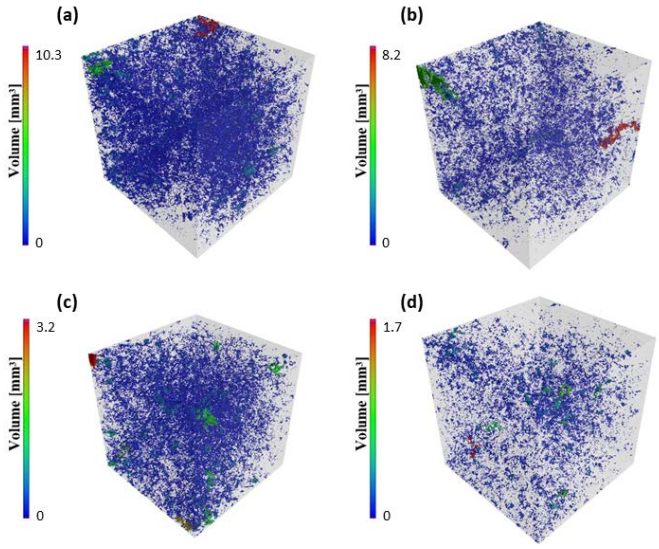

Fig. 4. XCT images of samples before(a.S1-5-R and b.S1-10-R) and after(c.S1-5-C and d.S1-10-C) carbonization curing.

The accumulated pore size distribution (APSD) and differential pore size distribution (DPSD) were analyzed and presented in Fig.5. For S0-5 sample, the curves of APSD and DPSD were close to zero when the pore diameter was greater than 1000 nm, manifesting that there were almost no pores in this range. However, when the FA/SSC ratio increased to 1 (S1) and 2 (S2), a cumulative distribution plateau (Fig. 5a) and a smaller distribution peak (Fig. 5b) appeared around 10 μm. This distribution peak was attributed to the fact that the FA content in samples was too large, and SWS particles were no longer able to fill the gaps between FA particles, resulting in more pores distributed around 10 μm.

After CM treatment, the critical pore (the peak of DPSD curve) distribution peak intensity of all samples decreased. This reduction was especially significant in S0-5-C sample, where the characteristic peak intensity decreased from 0.32 to 0.20, with a drop rate of 40%. The results indicate that the CM treatment to $Ca(OH)_2$ forms $CaCO_3$ that fills the pores between compacted particles, resulting in a decrease in the critical pore distribution peak intensity. Additionally, it is can be observed that the critical pore size of S0-5-C sample increased to about 300 nm (Fig. 5b). This is because the volume expansion of $CaCO_3$ may cause material to form connected micro-cracks, leading to an increase in the critical pore aperture size.

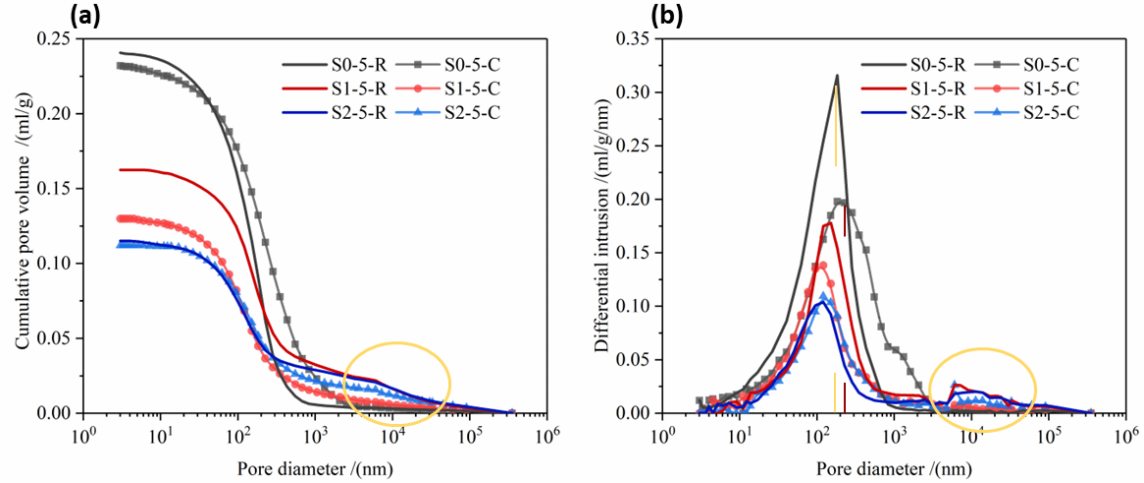

Fig. 5. (a) APSD and (b) DPSD of the samples before and after carbonization.

3.4 CO_2 emission assessment

The total CO_2 emissions E_S of project include the CO_2 emissions E_C from all net consumption of fossil fuel combustion activities, the CO_2 emissions E_{SC} produced by the industrial production process, and the CO_2 emissions E_W generated by the net purchase of electricity and heat (GB/T32150: 2015). Additionally, the SWS blocks produced in this study established strength by absorbing CO_2, so the amount of CO_2 absorbed C should be subtracted when calculating the E_S. The sources of carbon emissions and sink in this work are shown in Fig. 6. In summary, the E_S during production process was calculated using the following equation:

$$E_S = E_C + E_{SC} + E_W - C \quad (1)$$

The E_S of SWS blocks was calculated, and the results are shown in Table 3. The E_S of SWS blocks were relatively low. Except for S0-10 sample (216 kg e-CO_2/m^3), the E_S value of all other samples were lower than 160 kg e-CO_2/m^3, significantly lower than that of autoclaved fly ash-lime brick of 340kg e-CO_2 /m^3, clay bricks of 460-550 kg e-CO_2 /m^3 (GB/T 51366: 2019), and aerated concrete blocks of 232kg e-CO_2 /m^3 (He et al. 2020). The E_S of blocks increased with increasing pressing pressure. This is because higher pressing pressure results in the increased compactness of SWS blocks, making it more difficult for CO_2 to migrate to the middle of blocks and react with active $Ca(OH)_2$. This is supported by the XRD test results of S1-10 sample, which showed that there is basically no carbonization inside the block (Fig. 3).

Furthermore, under the same producing conditions, increasing the FA/SSC ratio can help reduce the CO_2 emissions of SWS blocks. The E_S value of S2-5 block was only 56.20kg e-CO_2/m^3, which is only about one third of that of S0-5 block. Because the increase of FA/SSC ratio reduces the amount of $Ca(OH)_2$ in the mix, thereby reducing the E_S value. However, increasing the FA/SSC ratio would reduce the consumption and utilization of SWS. Thus, based on the data in this study, controlling the FA/SSC ratio below 2 is recommended for the massive consumption of SWS.

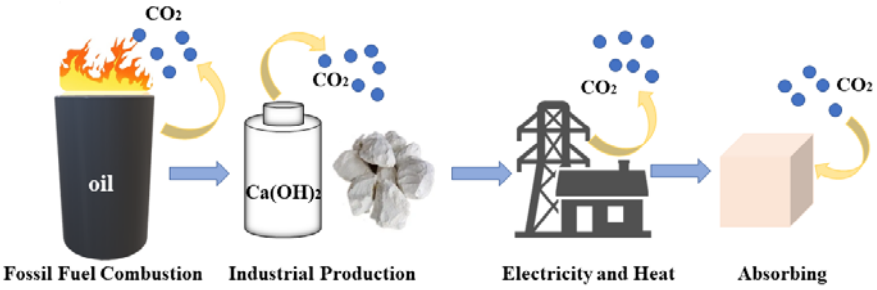

Fig. 6. Sources of carbon emissions and sink in this work.

Table 3. Carbon emissions of different types of blocks (kg e-CO_2/m^3).

Sample name	Ew	Esc	C	Es
S0-1	1.75	251.05	234.53	18.27
S0-5	1.75	283.28	128.58	156.45
S0-10	1.75	297.04	82.11	216.68
S1-1	1.75	165.44	119.01	48.18
S1-5	1.75	177.79	116.30	63.24
S1-10	1.75	185.61	69.86	117.50
S2-1	1.75	125.18	87.02	39.91
S2-5	1.75	130.50	76.05	56.20
S2-10	1.75	132.86	31.13	103.48

4 Conclusion

- The compressive strength of SWS blocks initially increased and then decreased with increasing the FA/SSC ratio, and achieved the highest strength (7.42 MPa) at a FA/SSC ratio of 1.
- CM can significantly improve the strength of SWS blocks, with a maximum increase of 215.7%.
- The E_S values of blocks produced by CM treatment are 18.27-216.68 kg e-CO_2/m^3, lower than those of other building blocks. Considering the balance between strength and CM degree, the optimum producing parameters of SWS blocks are the FA/SSC ratio of 1, and the forming pressure of 5 MPa.

Acknowledgements (optional)

The authors greatly thank the financial support from the National Natural Science Foundation of China (No. 51838004).

References

Abanades, J.C., Rubin, E.S., Mazzotti, M. and Herzog, H.J. (2017). *On the climate change mitigation potential of CO_2 conversion to fuels*. Energy & Environmental Science, 10(12): 2491-2499.

Chen, Z.C., Yang, Z.Y. and Li, Y.C. (2013). *Calculation method for carbon dioxide emissions in the production of sintered bricks and tiles*. Brick & Tile World, 91(02), 21-23.

Gajurel, A., Chittoori, B., Mukherjee, P.S. and Sadegh, M. (2021). *Machine learning methods to map stabilizer effectiveness based on common soil properties*. Transportation eotechnics, 27.

He, Y.Q. (2020). *Feasibility Study on Zero Carbon Residential Areas in Moderate Areas*. kunming university of science and technology.

Huang, L.C., Guo, X., Miao, H., Li, X. and Wu, F.F. (2022). *Decarbonization cost control for carbon neutrality: optimizing technological innovation and policies*. Studies in Science of Science, 40(12), 2187-2193.

Inasaka, K., Trung, N.D., Hayano, K. and Yamauchi, H. (2021). *Evaluation of CO_2 captured in alkaline construction sludge associated with pH neutralization*. Soils and Foundations, 61, 1699-1707.

Keykha, H.A., Romiani, H.M., Zebardast, E., Asadi, A. and Kawasaki, S. (2021). *CO_2-induced carbonate minerals as soil stabilizing agents for dust suppression*. Aeolian Research, 52.

Mi, J.F., Wang, H., Liu, J.B. and Yan, H. (2017). *Research and Application Progress of Soil Stabilizer*.

Puppala, A.J. (2016). *Advances in ground modification with chemical additives: From theory to practice*. Transportation Geotechnics, 9, 123-138.

Song, Q.F., Zhu, Z.J., Wang, J.X., Long, B.Y., Luo, W.S., Jia, Z.Q. and Wang, S. (2021). *Status Quo of Resource Utilization of Urban Engineering Dregs*. China Resources Comprehensive Utilization, 39(08), 90-92.

Sun, X.G., Zhu, S.S., Pan, T. and Li, H.N. (2022). *Studies on Effects of Carbonization on physical and mechanical Properties of Improved Expansive Soil*. Northwest Hydropower, 3, 39-44.

Wang, D.X., Zhu, J.Y. and He, F.J. (2019). *CO_2 carbonation-induced improvement in strength and microstructure of reactive MgO-CaO-fly ash-solidified soils*. Construction and Building Materials, 229.

Wang, F.J., Zhao, L., Liang, Y., Ma, G.P., Liu, H.H. and Yang, T.T. (2021). *Study on Mix Ratio Parameters of Solidified Soil Prepared from Construction Waste Residue*. Architecture Technology, 52(07), 801-804.

Wu, F., Gao, T., Wang, X.X., Cai, X.Y. and Jiang, C.F. (2021). *Experimental Study on the Effects of Forming and Maintenance Systems on the Physical Properties of Dredged Soil Blocks*. China Water Transport, 8, 116-118.

Yang, B.C. and Xu, G.D. (1985). *The excavation at Hougang in Anyang,1979*. Acta Archaeologica Sinica, 1, 33-88+134-145.

Zhang, J.J., Chen, j. and Dou, Y.H. (2023). *Research on resource utilization of urban construction waste*. Recyclable Resources and Circular Economy, 16(02), 17-20.

GB/T 51366-2019 (2019). *Standard for building carbon emission calculation*.

GB/T32150-2015 (2015). *General guideline of the greenhouse gas emissions accounting and reporting for industrial enterprises.*